Neutral Cesium Velocity Vector and Absolute Number Density LIF Optical Measurement with Application to a Flight Model MICROSCOPE Cesium FEEP Thruster

IEPC-2007-219

Presented at the 30th International Electric Propulsion Conference, Florence, Italy
September 17-20, 2007

Denis Packan*, Jean Bonnet†, Alexandre Bresson‡ and Brigitte Attal-Tretout§

ONERA, Chemin de la Hunière, 91120 Palaiseau, France

Abstract: An experimental setup for the optical measurement of neutral cesium flowrate in the plume of a flight model Cesium FEEP thruster, developed by ALTA for the MICROSCOPE mission, has been designed and tested. It allows to measure point-by-point, with a 1 mm spatial resolution, the absolute density of cesium atoms by Laser Induced Fluorescence and absorption spectroscopy, and the average velocity components of the atoms along three axis with Laser Induced Fluorescence. The setup has been successfully tested with a neutral cesium source, and results are presented. The accuracy of the measurements is about $2x10^7$ cm^{-3} in number density and 3 m/s in velocity.

I. Introduction

Micronewton Cesium FEEP thrusters are considered as the main propulsive system for space missions such as MICRSCOPE. One of the potential problems of such a thruster is contamination of the spacecraft by slow cesium ions. A FEEP thruster plume is composed mainly of fast ions, but some traces of neutral cesium are always present due to evaporation at the thruster tip or due to other processes. These slow neutral species in the plume may collide with fast ions and this leads generally to a charge exchange reaction, where the slow neutral atom is transformed into a slow ion. The slow ions then become trapped in the electric field of the satellite and may end up on sensitive surfaces such as solar panels, which will deteriorate with time due to the conductive and corrosive properties of cesium. Because the flowrates are so minute, it is a difficult to measure by weighting. For example, an estimate[1,2] of the evaporation rate of cesium atoms at the tip of the FEEP thruster gives $1.4x10^{12}$ s^{-1} or 9.5 mg/year, which is very challenging to measure with a weight scale given the mass of the thruster (> 1 kg).

However cesium has several interesting properties that point toward optical measurements. It has a very strong transition (the D2 transition, with a lifetime of 30.47 ns) that is linked to the ground state of the atom[3]. This means that the population of the atom can be probed optically. The transition is also very well known and the hyperfine levels were measured accurately, because it is a transition that is used for atomic clocks. Finally, the saturation vapor pressure of Cesium at room temperature is $2x10^{10}$ cm^{-3}, which is quite large given the strength of the transition and allows for a convenient absolute calibration.

It was thus proposed to probe optically the plume of the MICROPSCOPE flight model Cesium FEEP thruster, manufactured by ALTA, in order to measure the cesium atom flowrate. The experimental setup was prepared for the thruster, but test measurements were made on a cesium source, which is more flexible than an actual thruster. Such a source was found from SAES Getter S.p.A., which manufactures alkali dispensers for the semiconductor industry

* Research Engineer, Physics and Instrumentation Department, denis.packan@onera.fr.
† Research Engineer, Physics and Instrumentation Department, jean.bonnet@onera.fr.
‡ Research Engineer, Physics and Instrumentation Department, alexandre.bresson@onera.fr
§ Senior Research Engineer, Physics and Instrumentation Department, btretout@onera.fr

(reference CS/NF/16/50 FT10+10). The dispenser is a metal tube 2 mm x 2 mm x 70 mm with a longitudinal slit 100 µm x 50 mm. When heated by a flowing current, the cesium dispenser releases pure, gaseous cesium along a its longitudinal slit. It releases a plume of neutral cesium, supposedly near room temperature, which can be probed by our optical setup instead of the thruster plume.

Figure 1. Close-up view of the dispenser slit.

The test measurements on the cesium dispenser, composed of 8 point measurements of absolute density and velocity vector along the dispenser slit, are presented in this paper. Measurements on the actual flight model FEEP thruster are planned in the near future.

II. Principle of flowrate measurement

The flowrate that will be measured on the FEEP thruster is calculated by integration of the Cesium atoms flux across a surface enclosing the plume. The integration is a sum of the local fluxes determined by measuring the number density and velocity vector of cesium atoms. The shape of this surface will be determined in order to encompass the majority of the plume. An expression for the flow-rate is

$$F = \iint_{surface} n \cdot \vec{\bar{v}} \cdot d\vec{s}$$

where

F [s^{-1}] is the flow-rate of neutral Cesium atoms

n [m^{-3}] is the measured number density of Cesium neutral atoms

$\vec{\bar{v}}$ [$m.s^{-1}$] is the measured average velocity vector of the neutral atoms

$d\vec{s}$ is the outgoing surface vector.

A more accurate formula makes use of the velocity distribution:

$$F = \iint_{surface} n \cdot \underbrace{\left(\iiint f(\vec{v}) \cdot \vec{v} \cdot dv_x \cdot dv_y \cdot dv_z \right)}_{\vec{\bar{v}}} \cdot d\vec{s}$$

with $f(\vec{v}) = f(v_x, v_y, v_z)$ the normalized distribution (its integral equals unity).

What is measured during the experiment is really the distribution of velocity components f_x, f_y and f_z along three axis: they correspond to the three lineshapes respectively measured on the three laser axis. They are related to f by:

$$f_x(v_x) = \iint f(v_x, v_y, v_z) \cdot dv_y \cdot dv_z$$

$$f_y(v_y) = \iint f(v_x, v_y, v_z) \cdot dv_x \cdot dv_z$$

$$f_z(v_z) = \iint f(v_x, v_y, v_z) \cdot dv_x \cdot dv_y$$

From the measurement of f_x, f_y and f_z one can calculate the mean velocity components, which are also equal to the components of the mean velocity vector:

$$\overline{v_x} = \overline{\vec{v}_x} = \int f(v_x) \cdot v_x \cdot dv_x$$

$$\overline{v_y} = \overline{\vec{v}_y} = \int f(v_y) \cdot v_y \cdot dv_y$$

$$\overline{v_z} = \overline{\vec{v}_z} = \int f(v_z) \cdot v_z \cdot dv_z$$

The flowrate $F = \iint_{surface} n \cdot \overline{\vec{v}} \cdot d\vec{s}$ is then deduced.

Although we are able to extract the local distribution of velocity components $f_x(v_x)$, $f_y(v_y)$ and $f_z(v_z)$, and consequently the mean velocity vector and the flowrate from the experimental results, we will not be able to extract the local distribution of velocity vectors $f(v_x, v_y, v_z)$. Note that one can see written sometimes:

$$f(v_x, v_y, v_z) = f_x(v_x) \cdot f_y(v_y) \cdot f_z(v_z)$$

This is not true in the general case (although it is true for a Maxwellian distribution), and more particularly it is not true in our case.

Flowrate measurement were not made in the case of the cesium dispenser.

III. Spectroscopic properties

The D2 transition of Cesium at about 852.3473 nm is detailed in Figure 2. Historically, people have noticed its two key advantages: it is very intense and it starts from the ground state. The intensity ensures that excitation does not require prohibitively-powerful light sources. And starting from the ground state ensures that the total population of atoms is probed. If one takes a transition starting from an excited state instead, only the small fraction of population in that excited state is probed. This would yield a low intensity of emission and absorption that would not be easily related to the actual number of atoms.

One other property is that the D2 transition is "isolated": the upper state is radiatively linked only to the ground state. Note that the total pressure in the plume during the experiment will be lower than 10^{-6} mbar, so the mean free paths of atoms is kilometers long, and we can thus assume that there is no collisions at the point of measurement. We can ignor quenching, and the transition can be considered close to an ideal two-state system. This and other properties made cesium used in atomic clock, which resulted in numerous studies of the D2 transition and its characteristics are now very well known. It also resulted in the availability of off-the-shelf lasers at its wavelength (about 852 nm). For all these reasons, the D2 transition is ideal to make quantitative measurements on cesium atoms.

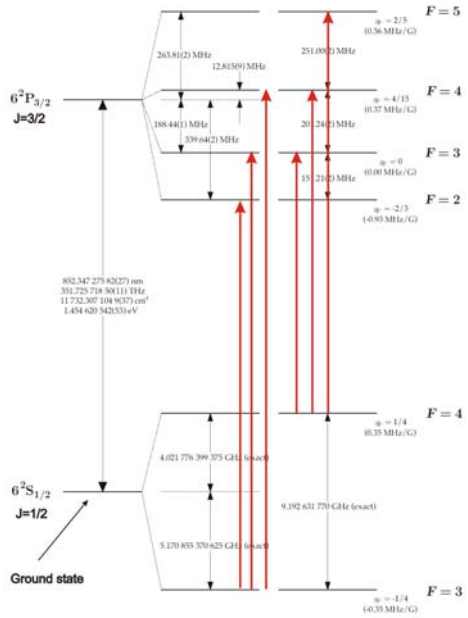

Figure 2. Allowed transitions between fine levels of the D2 transition of Cesium.

There are two lower states and four upper states. The two lower states are 9.2 GHz apart, and since we are working close to room temperature both lower states will be equally populated. The upper state splitting is about 200 MHz, which is the same order of magnitude as the Doppler broadening at room temperature, so the components will not be seen individually (this is taken into account during data analysis). The absorption and emission spectra will thus be composed of two groups of three overlapping, Doppler-broadened transitions 9 GHz apart.

It has also been checked that Stark shift of the energy levels due to the electric field of the FEEP thruster, and the Zeeman shift due to the local magnetic field are negligible.

For reference, the natural linewidth of the transition is 5 MHz and the linewidth of the CW diode laser used is about 1 MHz.

IV. Vacuum facility

The vacuum facility is composed of a vacuum tank 4 meters in length and 1 meter in diameter, attached to an auxiliary chamber 1 meter in length and 60 cm in diameter with optical viewports (Figure 3), where the thruster will be located. In between is a gate valve 50 cm in diameter. The auxiliary chamber has a turbopump of 2000 l/s pumping speed (but only 1000 l/s for Cesium), and the main tank has a cryogenic pump (minimum temperature about 35 K) of 8000 l/s pumping speed for Cesium. These pumps can maintain a vacuum level of less than 10^{-6} mbar (possibly 10^{-7} mbar, depending of the outgassing of the optical bench installed in the tank) when the thruster is not running. 10^{-7} mbar has been achieved in an empty vacuum tank. The tank is fitted with a mass spectrometer.

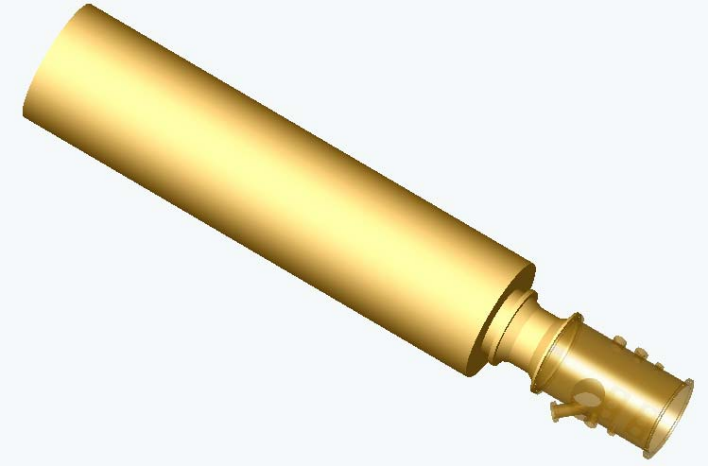

Figure 3. Simplified CAD view of the vacuum tank at ONERA. The auxiliary chamber is on the right.

V. Optical setup

Since we measure the velocity components along the laser beam axis in Doppler-LIF experiments, 3 laser beams will be used for LIF, in order to get the full velocity vector. The beams will be used one at a time. They form an orthogonal trihedron (they are all perpendicular to each other), although other orientations may be used but would require more trigonometric conversions. Ideally one laser beam should come from the front of the thruster. However it was chosen to avoid putting any optics in the thruster plume, because the energetic cesium ions would deteriorate it quickly. All the optics that are positioned downstream from the plume are on the periphery, looking at an angle, including the laser beams. Trigonometric transformations are needed to find the velocity vector in the horizontal frame of reference of the thruster.

The optical components of the experiments have been separated in two groups. One group is inside the vacuum tank and is made of injection and detection optics (lenses). It is placed as close as possible from the plume to maximize the signal, and with angles of view that could not be provided by viewports. It will be illustrated in the section on the principle of operation. The second group is outside the tank and is made of the laser beam conditioning and monitoring optics and the detection electronics. Optical communication between the two groups is made via optical fibers and vacuum feedthroughs. Indeed at 852 nm optical fibers can transmit light for 100s of meters without significant attenuation. The diameter of the fiber was chosen to allow easy coupling with the laser and sufficient spatial resolution on the plume.

The outside optical layout for LIF and absorption measurements is shown in Figure 4.

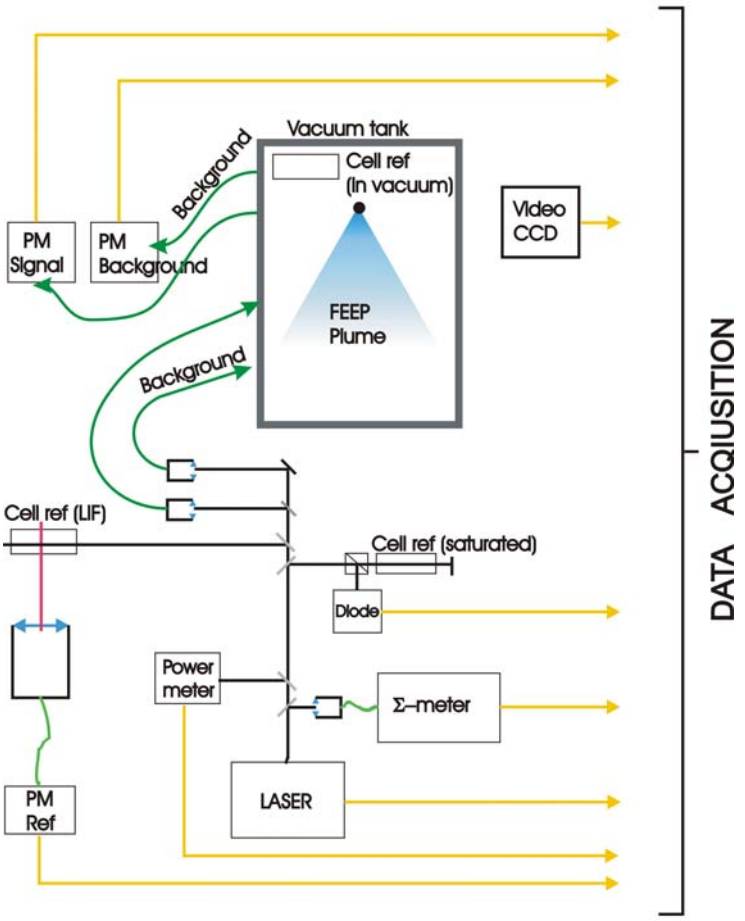

Figure 4. Optical layout of the optics outside the vacuum tank for LIF and absorption measurements. "PM" stands for "Photomultiplier Tube".

The laser source is a Sacher Lasertechnik TEC500 with a power up to 20 mW and a modhop-free tuning range of about 10 GHz and a linewidth on the order of 1 MHz. This means that we can detect velocities up to about 10 km/s in one scan. The laser is controlled with a voltage, but the calibration voltage versus wavelength is not known or repeatable. Therefore we need ways to determine the wavelength. For large Doppler shifts (greater than 1 GHZ or 1km/s) we can use a wavemeter that measures directly the wavelength. Its precision is about 70 MHz. For Doppler shifts smaller than 1 GHz, ie for thermal velocities, we will use frequency markers created in a reference cesium cell with the so-called saturated-doppler technique, or saturated-absorption technique, which consist in passing a beam back over its own path in a cesium cell, and observing the absorption signal. Without entering into the details, there appear sharp peaks of reduced absorption (or "holes") in the spectrum at wavelength precisely known. These can be used as frequency markers to calibrate the wavelength. This wavelength calibration procedure is illustrated in Figure 5.

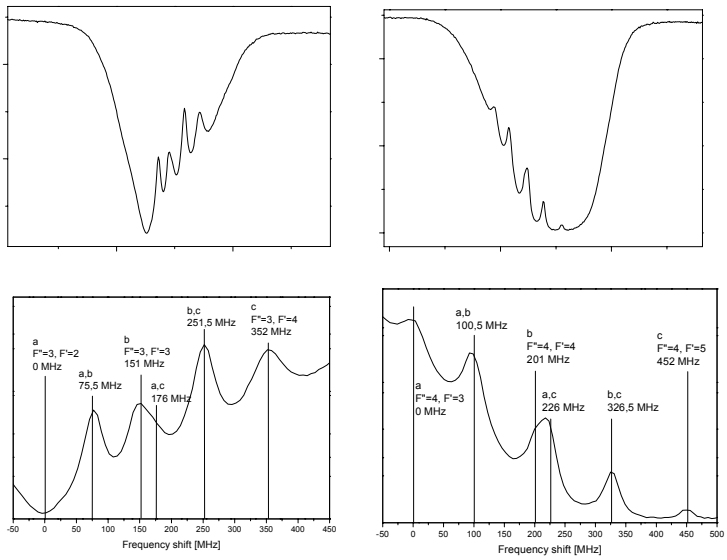

Figure 5. Positions of the holes in Doppler-free absorption from the F"=3 state (left) and from the F"=4 state (right) of the D2 transition of cesium, superimposed on measured Doppler-free spectra (shown in their entirety in the top graphs).

The laser power will also be controlled and, for reference, a cesium cell will be used to get an LIF signal. Finally the laser signal is split in two for the two optical inputs into the vacuum tank: one for signal injection, and one for background cesium monitoring (see Figure 14).
The background and LIF or absorption signals coming back from the experiment are analyzed with photomultiplier tubes that are sensitive in the near infrared.

VI. Optical bench and principle of operation

All the mechanical elements used on the optical bench installed in the vacuum tank, including the translation stages, the optical mounts and the motorized optical mounts, are vacuum rated. In all the following drawings, the laser beams appear as red lines and the detection cones are materialized as red cones.

A general view of the optical bench is provided in Figure 6. Individual elements are detailed and shown afterwards.

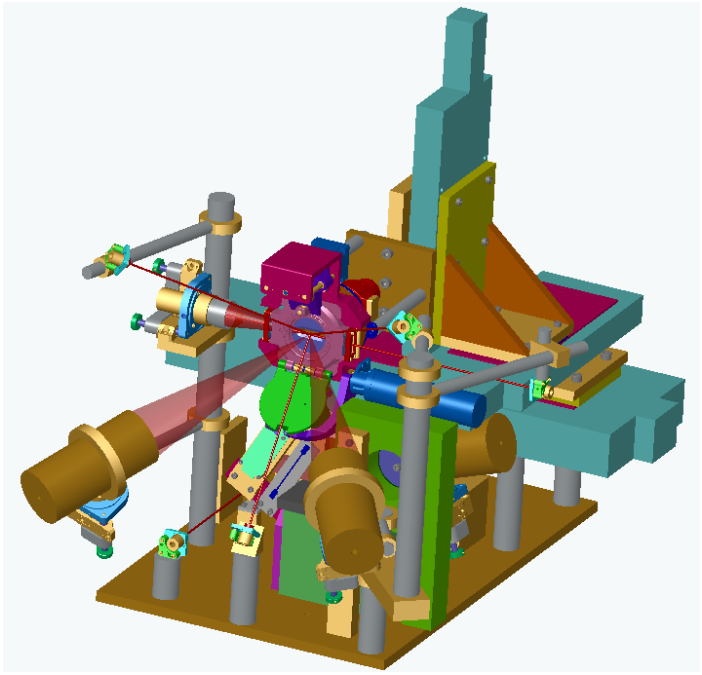

Figure 6. 3D CAD view of optical bench with a FEEP thruster mounted.

The FEEP thruster will be mounted on three translation stages with 10 μm accuracy that will allow it to perform the spatial scans. The translating system is shown in Figure 7. All the optics will be fixed (except for some minor adjustments allowed by the motorized mounts) and the only movement will be that of the FEEP thruster. Because of the complexity of the setup and the constraints of the vacuum tank, it was designed in 3D using the CAD software Solidworks.

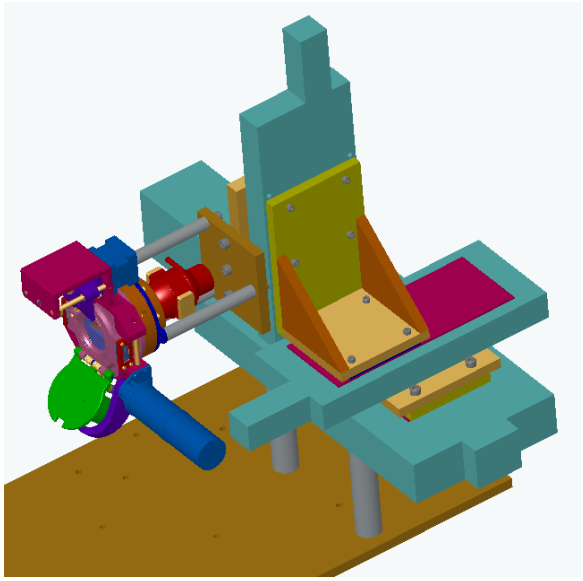

Figure 7. CAD view of the FEEP thruster mounted on the translation stages.

The laser beams used for LIF are arranged into an orthogonal trihedron in order to easily provide the velocity vector of the cesium atoms. It is represented in Figure 8. As already mentioned no optics is placed directly into the ion beam to prevent deterioration due to ion impact, thus the trihedron is placed at an angle, with is axis of symmetry along the axis of the thruster.

The three detection modules used for LIF are shown in Figure 9. They all have approximately the same solid angle: 5 cm in diameter placed 20 cm away (left and right detection modules), or 2.5cm diameter placed 10 cm away (lateral detection module). The detected light is carried out of the vacuum tank with optical fibers 600µm in diameter (nor represented on the drawings). The optics used for the absorption measurements are shown in Figure 10.

Alignment and calibration will be done using 3 elements mounted on a swinging arm controlled by a rotation stage (Figure 11).

- a CCD camera will define the measurement plane. When it is in place, its image will show the impacts of the laser beams from the injection modules and from the back-tracked detection modules to check their superposition;
- a cesium dispenser will be used to create a cesium gas in which to optimize the alignment of laser beam and detection;
- a calibration cell will be used for absolute calibration of the LIF signals.

Figure 11 shows the system for alignment and calibration. During its operation, the thruster is backed up by 100 mm. The box with green, purple and grey walls at the bottom of the view is hiding the calibration cell. In order to avoid contamination by sputtering during thruster operation, the calibration cell is kept in this box which opens itself up when the rotation stage moves into action. This ensures that absolute LIF calibrations do not deteriorate with time.

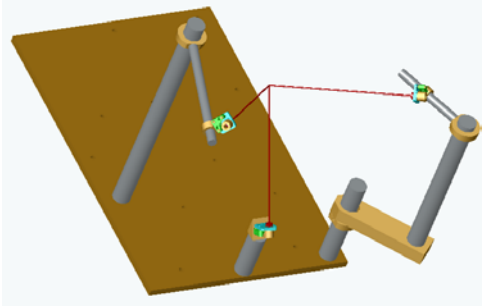

Figure 8. CAD view of the three laser beams used for LIF. Optical fibers bring the laser light to the injection modules (fibers not represented).

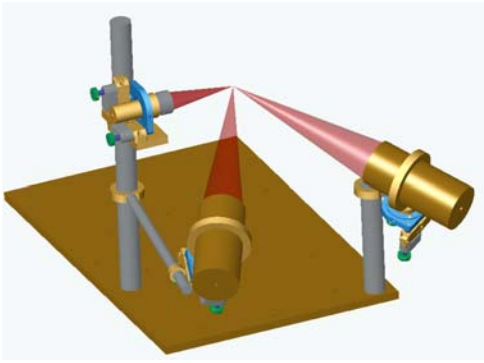

Figure 9. CAD view of the three detection modules that can be used for LIF measurements. The cones of detection are materialized in red.

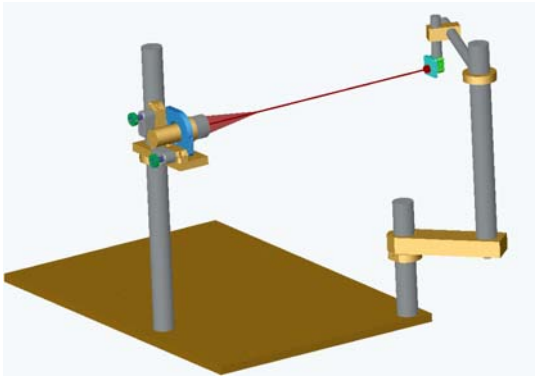

Figure 10. CAD view of the laser injection module and the detection module used in absorption measurements.

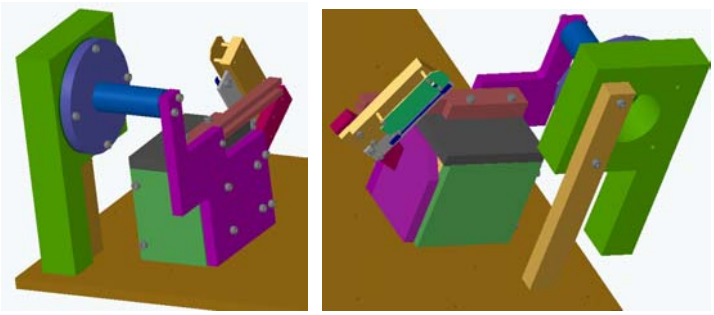

Figure 11. Back view (left) and front view (right) of the alignment and calibration system, featuring the rotation stage (apple green), the swinging arm (purple), the CCD (light green), the cesium dispenser (dark blue) and the closed "box" protecting the calibration cell.

The operation of the system is shown in Figure 12. First the CCD is put at the optical center of the optical bench, then the cesium dispenser, and finally the calibration cell. A view of the calibration cell in place within the optical bench is shown in Figure 13.

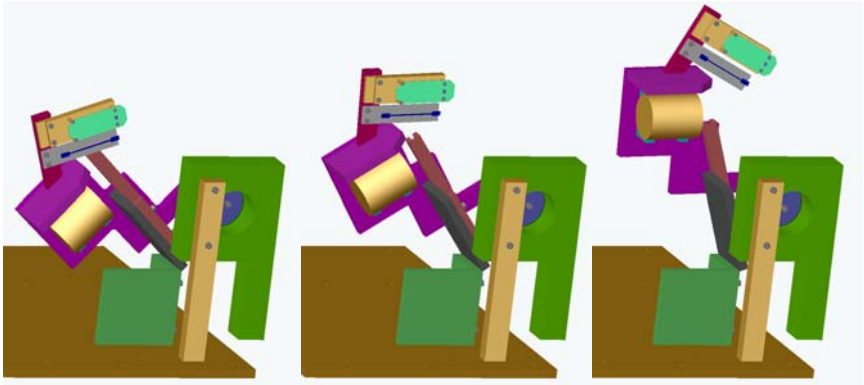

Figure 12. Operation of the alignment and calibration system. The three main positions of the swinging arm are shown. It places in the measurement beams (not represented here) successively the CCD chip (left), the dispenser (middle) and the calibration cell (right).

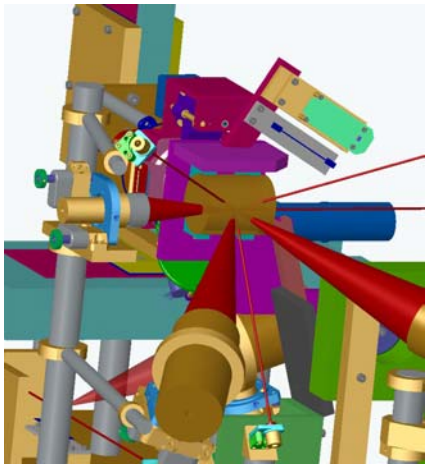

Figure 13. View of the optical bench with the calibration cell in place. The thruster is backed up by 100 mm.

In order to monitor the background number density of thermal cesium atoms in the auxiliary tank, a set of injection module/detection module for LIF detection is installed in the optical bench below the thruster. It is shown in Figure 14.

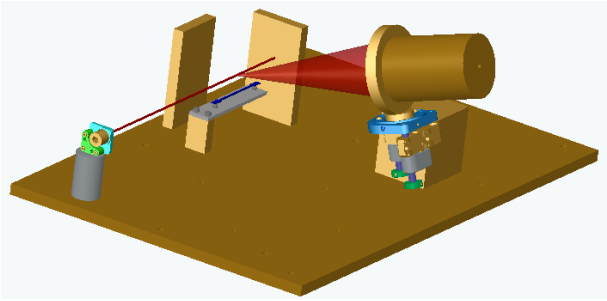

Figure 14. CAD view of the background cesium LIF control setup, with the injection module, the detection module and the cesium dispenser used for alignment.

The detection module is aligned on the laser beam and looks at the LIF signal from the background gas. A cesium dispenser is placed close to the measurement point so that the detection module can be aligned (using its motorized optical mount) on the laser beam using the LIF signal from the cesium gas created. Because of the position and orientation of the optics used, they are immune to ion etching or tank wall sputtering, thus in the course of the experiments the LIF signal obtained will be proportional to the density of background cesium gas present. Although no absolute measurement is planned, the LIF signal could be directly compared to the LIF signal from the plume because the optics and detector used are the same. Another method for Cesium background control is the mass spectrometer of the vacuum tank.

VII. Experiment and results

The full experimental setup was used to measure a longitudinal profile of number density and average velocity vector, with both LIF and absorption technique, on a cesium dispenser placed in place of the FEEP thruster. The line along which the measurement was made was parallel to the dispenser, and positioned about 3 mm downstream from the dispenser. The dispenser used is 7 cm long, and 8 measurement points were taken across these 7 cm (ie one point every centimetre). At each point the three LIF laser beams were successively used, and then the absorption beam was used. The current through the dispenser was 4 A. The main signal was recorded along with, simultaneously, the background signal from the optical background system, the reference LIF signal from the cesium cell on the optical

table, the Doppler-free signal giving the wavelength references, and the laser intensity. A picture of the dispenser mounted in the optical setup is shown in Figure 15.
During all experiments, the total pressure in the vacuum tank was about $3x10^{-7}$ mbar with a partial O_2 pressure of $3x10^{-8}$ mbar and a partial pressure in H_2O of $9x10^{-8}$ mbar.

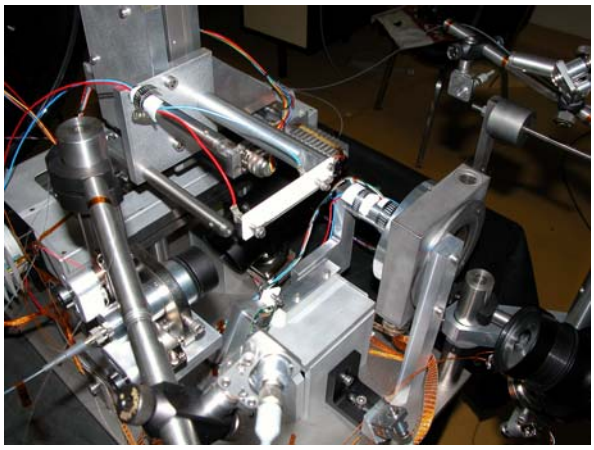

Figure 15. Picture of the dispenser mounted on the optical bench.

The alignment CCD was used to image the laser beams from the injection modules and from the back-tracked detection modules. Before closing the vacuum tank, the CCD images (video) were used to check that the spatial resolution of both the injection and detection modules is about 1 mm, and that they are aligned. After vacuum is established in the tank and prior to each experiment, the CCD is used to check the alignment of the optics. The motorized optical mount on the detection modules were used to enforce alignment after the setup has settled down in the vacuum. The mounts were also used for the slight adjustment needed for maximization of the signal in the alignment dispenser (although with a dispenser in place of the FEEP thruster, the alignment dispenser is redundant). The images of the alignment beams on the CCD are shown in Figure 16.

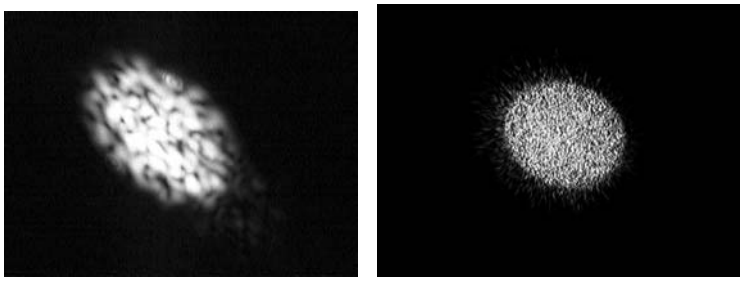

Figure 16. Images of the impact on the alignment CCD, of the laser beam from the injection module (left) and back-tracked detection module. During alignment in vacuum, the images can be seen both at the same time and be made to superimpose.

The LIF signals were recorded at the 8 positions and are shown in Figure 17.

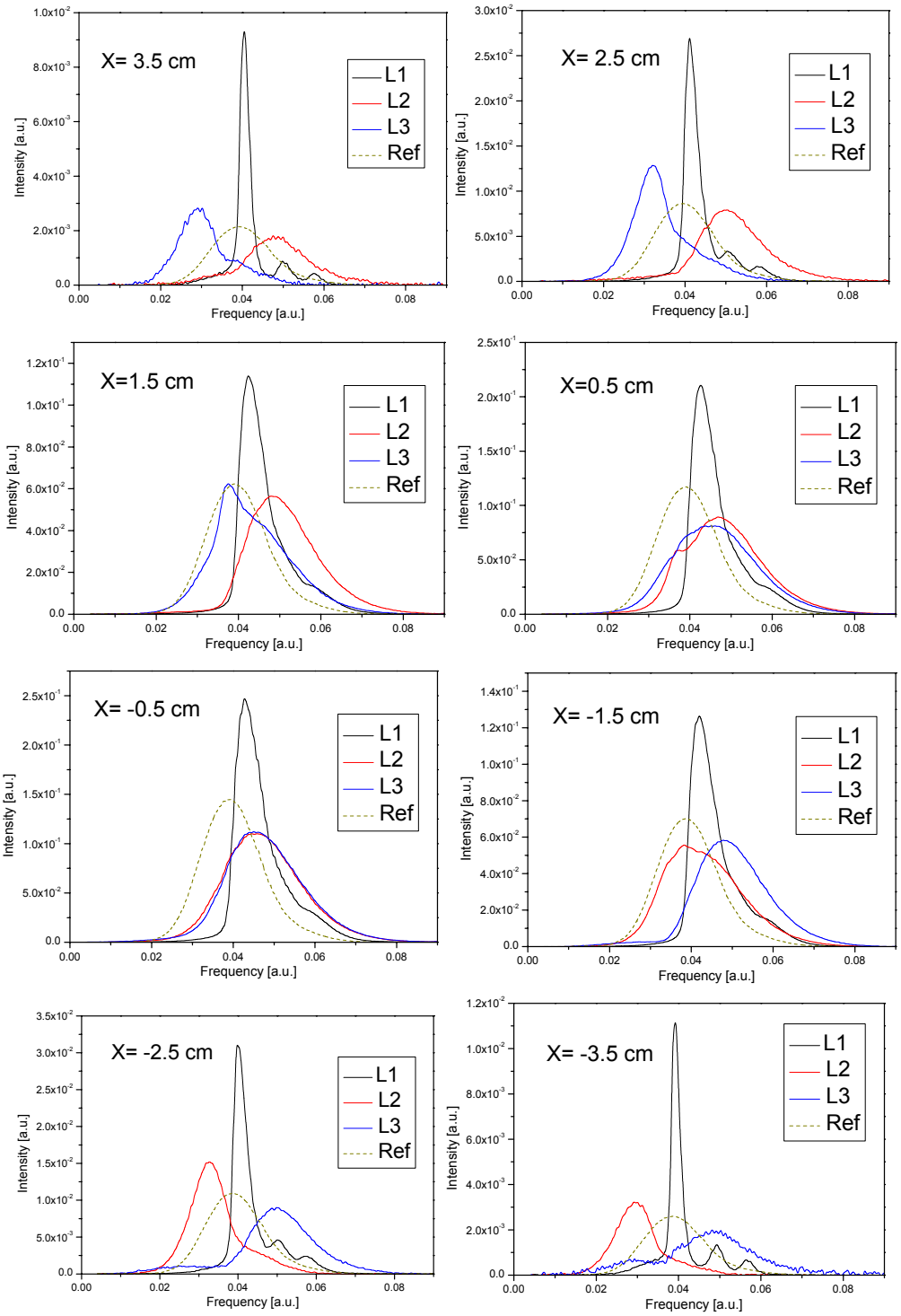

Figure 17. LIF signals obtained at the 8 spatial positions for the three laser axes and for the reference cell (with zero average velocity). The integral of the profiles within a plot are all equal.

The absorption signals obtained in the plume and the reference cell are shown in Figure 18.

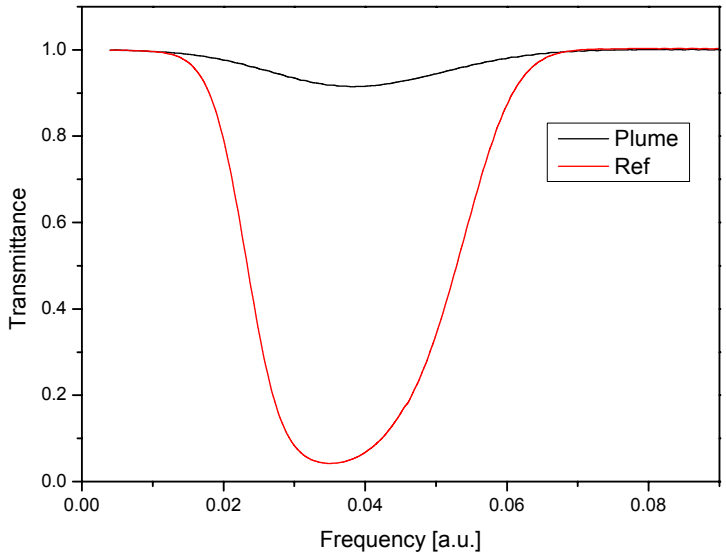

Figure 18. Signal from absorption as a function of laser frequency, for the plume (black) and the reference cell (red).

The algebra used to extract the number density and velocity from the measurements is texbook and will not be detailed here, although care should be taken when deriving the expressions, taking into account the doppler broadening and splitting of the levels.

The number density profile was determined using LIF, and it was calibrated with the absorption measurements. The density profile is shown in Figure 19. When a comparison was initially made between the absolute number density measured by LIF and the absorption measurement, it was found that the absorption was about 2.5 times higher than that measured by LIF. Because LIF needs an absolute calibration in the reference cell, it is possible that some aspects of the experiments prevent absolute calibration. The fact that the LIF signal calculated in the plume is too high indicates that the signal measured from the calibration cell was too low. Two possible explanations were thought of:

- lens effect by the glass of the cell itself: the glass cylinders defocuses the light
- self-absorption in the cell (although this would probably be to a lesser extent).

These are issues that are not easy to solve simply: one would need to design and manufacture a complex-shaped calibration cell with integrated cooling.
But this can be avoided, because we do not need the LIF absolute calibration: it is done anyway by the absorption measurement. In fact this is a standard procedure in optical diagnostics: measure a relative profile with LIF and calculate its absolute values using an absorption measurement.

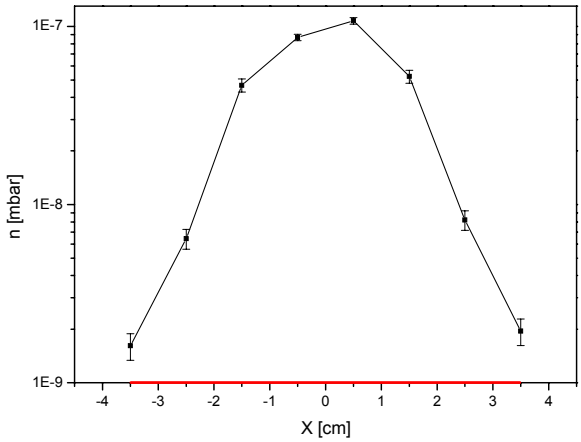

Figure 19. Absolute number density profile of cesium atoms in the dispenser plume measured by LIF and absorption. The estimated error bars are shown. The red bar indicates the dispenser size.

The average velocity vector at each position was calculated next using LIF data, The fixed coordinate systems used in our experiments are shown in Figure 20. The red frame is constituted by the three laser axes. The black frame is constituted by the axes of the three translation stages.

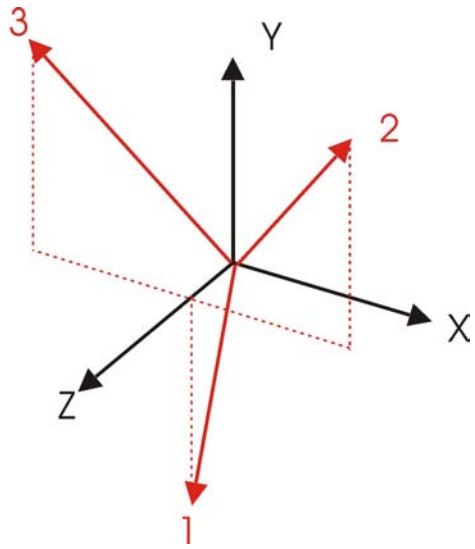

Figure 20. The two orthonormal reference frame vectors: fixed frame (black) and laser frame (red).

The distributions of velocities actually measured are f_1, f_2 and f_3 (yielding the local mean velocity vector and the local flowrate) instead of f_x, f_y and f_z.
(V1,V2,V3) was obtained and was converted with trigonometric relations into (Vx, Vy, Vz). The results are shown in Table 1.

X [cm]	V1	V2	V3	Vx	Vy	Vz	V
-3,5	11,72	224,50	-170,20	279,09	12,60	38,12	281,97
-2,5	56,77	288,77	-139,23	302,64	14,70	119,12	325,57
-1,5	123,29	282,03	101,64	127,55	55,97	292,69	324,14
-0,5	126,00	265,76	182,41	58,94	80,09	331,50	346,09
0,5	138,59	197,87	218,75	-14,77	56,92	320,55	325,90
1,5	121,42	101,66	269,67	-118,80	52,46	284,49	312,73
2,5	63,92	-112,45	256,00	-260,54	6,41	119,78	286,82
3,5	12,17	-143,25	195,84	-239,77	11,53	37,39	242,95

Table 1. Velocity vector coordinates and total velocity, in meters per second, on the laser frame and the reference frame at each of the 8 positions.

From this table it was possible to compare with the absorption measurement, and the agreement is about 10%.
The velocity vectors measured are shown projected on the (X,Z) plane in Figure 21.

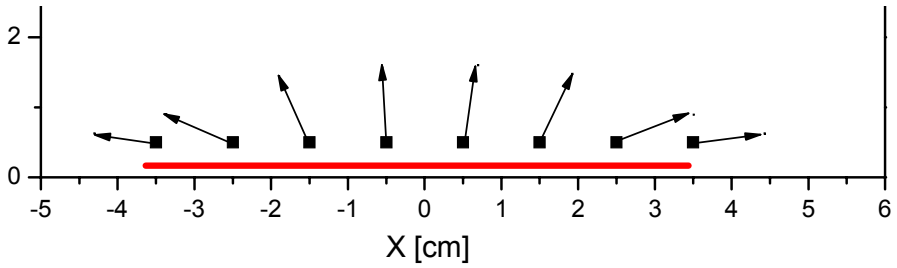

Figure 21. Illustration of the velocity vectors in the (X,Z) plane. The dispenser is shown as the red bar. The scale of the vectors is 300 m/s for one unit of axis.

The components in the Y direction are rather small, confirming that the probed points were nearly at the same Y position (ie height) as the slit.
The profiles of number density and velocity vector both show that most of the cesium is emanating from the central part of the dispenser. This is because the center of the dispenser gets to a higher temperature than the edges when the 4 A of heating current flows. The reason is that the electrical contact at the edges acts as a heat sink that drains heat from the dispenser. This could actually be observed: the imaging cameras used to monitor the dispenser were sensitive to the near infrared, they could see the glow of the heated dispenser and they distinctly showed that the center part of the dispenser was hotter.
Another observation is that the velocity vector is nearly parallel to the dispenser at its edges (again due to the fact that only the center of the dispenser emits). Without going into the details, we can say that this in fact explains the multi-peak appearance of the LIF signal at ±3.5 cm on Laser 1, where the three transitions are actually individually visible due to the small extent of the velocity spread along the axis of Laser 1. This correlation between the vector field and the distribution function is also a further confirmation of the accuracy of the measurements.

VIII. Conclusion

An experimental setup for the optical measurement of neutral cesium flowrate in the plume of a flight model Cesium FEEP thruster, developed by ALTA for the MICROSCOPE mission, has been designed and tested. It allows to measure point-by-point, with a 1 mm spatial resolution, the absolute density of cesium atoms by Laser Induced Fluorescence and absorption spectroscopy, and the average velocity components of the atoms along three axis with Laser Induced Fluorescence. The setup has been successfully tested with a neutral cesium source. The accuracy that was inferred from the measurements is about 2×10^7 cm^{-3} in number density and 3 m/s in velocity. A flight model

Cesium FEEP thruster should be delivered soon to us by ALTA, and the measurement on the thruster are planned next. The measurement of the cesium flowrate will be compared with a weighting of the thruster.
Since a large portion of cesium atoms may appear in the form of clusters, a test of clusters detection in the plume will be made, using a combination of Rayleigh scattering and fluorescence scattering.
Other measurements will also be undertaken on the thruster. Optical emission will be investigated, along with possible LIF on the cesium ions for velocity measurements.
Finally, let us point that the method used here for cesium FEEP thrusters could be extended to other thrusters, such as Indium FEEP thrusters and cold gas thrusters (preliminary investigations are ongoing).

Acknowledgments

We would like to acknowledge ESA for their financial support, and ALTA for their collaboration during the study.

References

[1] Spurio, M., "*Development and Supply of a Field Emission Electric Propulsion (FEEP) System for Microscope"*, ALTA SpA, 2004.
[2] Andrenucci M., Saverdi M;, and Saviozzi M., "*1000 h Endurance Test of a 150 μN FEEP Microthruster*", in Workshop on "Micro Propulsion for Spacecraft". CNES, Toulouse, 2004
[3] Steck, D. A., "*Cesium D Line Data",* Los Alamos National Laboratory, Los Alamos, 1998